Imaging Heterogeneity Of Soil By Means Of Geophysical And Geotechnical Investigation: In The Alluvial Plain Of Beirut

N. SALLOUM, D. JONGMANS, C.CORNOU, C.VOISIN & A.MARISCAL
ISTerre, Grenoble University, CNRS, IRD, IFSTTAR, Grenoble, France

D. YOUSSEF ABDEL MASSIH
Notre Dame University NDU, Louaize, Lebanon

F. HAGE CHEHADE & M. HAMMOUD
Lebanese University, Hadath, Beirut, Lebanon

SUMMARY
Site-specific geotechnical data are always random and variable in space. Geophysical methods are now increasingly used for sub-surface imaging. Geophysical and geotechnical tests were carried out in a site in Beirut (Lebanon). The survey included 2 electrical tomography profiles and ambient vibration measurements using 2 passive seismic arrays with different apertures. Geological and geotechnical information was obtained at 14 boreholes including SPT tests. Results show the strong lateral and vertical heterogeneity of the site, along with the relations between the geology, the geophysical parameters and the geotechnical properties (SPT). A procedure for quantifying the horizontal and vertical variability in geotechnical and geophysical characterization is also discussed to determine the correlation model to use for characterizing the spatial variability of Vs, SPT and resistivity obtained from geophysical and geotechnical tests.

Keywords: standard penetration test, spatial variability, shear wave velocity, electrical resistivity, Lebanon.

1. INTRODUCTION

The geological structure of Lebanon, a prone-to-earthquake country, is complex and heterogeneous at different scales of description (Dubertret, 1944, Abdallah, 2007), leading the seismic hazard and slope stability studies complex to perform. In this case, using deterministic average values in geotechnical engineering design may be considered unrealistic as this does not account for uncertainties related to the natural spatial variability of soil properties. Consequently, a more rational approach to geotechnical design is made possible by use of statistically based techniques of data analysis (Popescu, 1995) since it allows modeling the randomness and variability of the soil medium. The effects of spatial variation on a geotechnical system have been examined in previous studies. For example, Popescu et al. (1997) looked at the effect of soil spatial variability on soil liquefaction. Cho (2007) have established a probabilistic assessment of slope stability based on the spatial variability of soil properties. Recent advances in probabilistic simulation have considered modeling the seismic wave propagation in heterogeneous media (finite difference, spectral analysis, etc.) and applied it to the slope stability problem (Youssef Abdel Massih et al., 2009). Jaksa et al. (1997) modeled the spatial variability of the undrained shear strength of clay soils. The current obstacle is the construction of reliable geotechnical 2D/3D models that accounts for the spatial variability of soil properties. Geophysical methods are being increasingly used for imaging the subsurface for site effect and landslide studies (Jongmans and Garambois, 2007), because they are non invasive and fast to perform. However, measured geophysical parameters (e.g. compressional and shear waves velocities, electrical resistivity) cannot be directly exploited by the geotechnical engineers to perform calculations of strength or stability, which imply the knowledge of the cohesion and friction angle. For some applications (e.g. ground densification, liquefaction potential assessment), Vs alone, or in combination with Vp, could be empirically related to some geotechnical parameters like the porosity or the penetration resistance (Foti et al., 2002; Finn, 2000). This characterization of soil mechanics is usually obtained from expensive and destructive geotechnical tests and is limited to a small volume that can be investigated, either *in situ* (SPT, CPT tests …) or in the laboratory. The two families of techniques are then complementary and numerous relationships between geotechnical and geophysical parameters

have been proposed, mainly between the shear wave velocity Vs and penetration resistance N (Andrus *et al*. 2004; Hasancebi and Ulusay, 2007), although some attempts have been made to correlate SPT results and electrical resistivity ρ (Oh and Sun, 2008). The objective of this work is to exploit the geophysical (ρ and Vs) and geotechnical (SPT) parameters measured on an alluvial site in the city of Beirut, and to assess the capabilities of geophysical imaging methods to constrain the spatial variability of geotechnical characteristics.

2. SITE DESCRIPTION

The site is located at area called Korniche Al Naher, plain of the river of Beirut (fig. 1.). The Lot No. 4748 in Achrafieh is around 13500m² with irregular shape (fig. 2.). The area displays a relatively horizontal slope and flat relief. The formations exposed on the site and its vicinity belongs to the

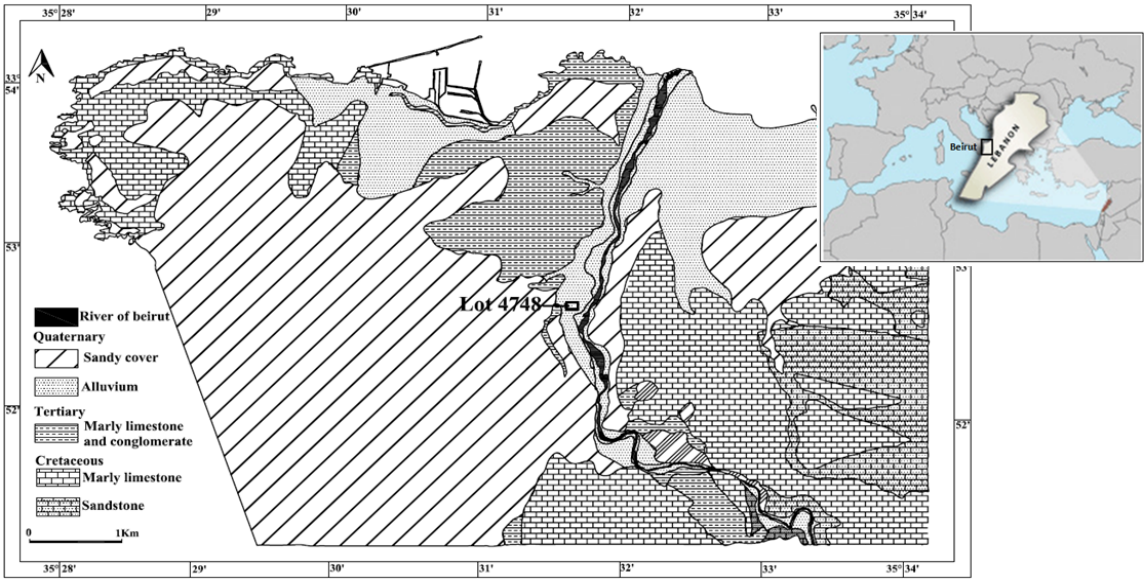

Figure 1. Simplified geological map of Beirut with the site location.

Quaternary deposits of Nahr Beirut. They are composed of alluvial sands (a few tens of meters) with a variable percentage of clay and fines. The quaternary deposits will include in places some rounded to sub-rounded fragments (class of Basalt, Chert, Limestone, and Dolomite) derived most probably from the river. The Quaternary deposits in the area are reddish to dark brown in color. They are overlying the Miocene formations and limestone which is of Cenomanian age (Dubertret, 1944). The construction of three buildings has been planned on this site and nineteen boreholes, 25 to 50 m deep, were drilled in 2008 and 2009 (see location in Fig. 2.). Standard penetration tests (SPT) were performed in these boreholes and the penetration resistance (number of blows: N) was measured every 1.5 m. The water table was encountered at a depth of 5 to 7 m below the ground surface, depending on the season. Geophysical tests were conducted in February 2011 during the

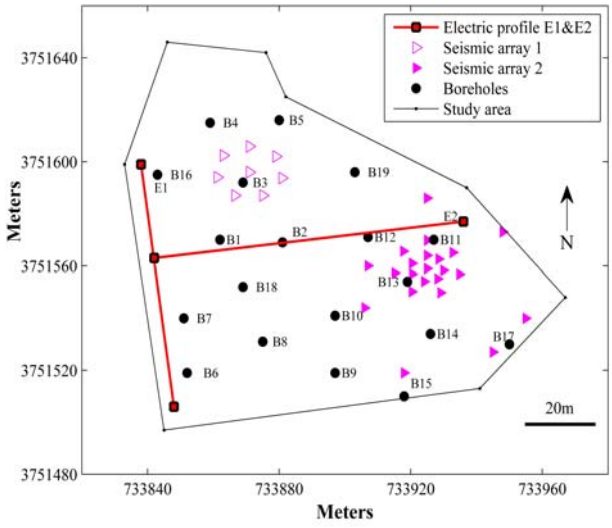

Figure 2. Site map showing the location of the 19 boreholes (B1 to B19), the 2 electrical profiles (E1 and E2) and the two seismic arrays 1 and 2.

excavation. Two electrical profiles of 94.5 m long (E1 and E2, Fig. 2.) were performed on a horizontal surface located 5 m below the natural ground level. The acquisition was performed using an ABEM Terrameter resistivimeter, deploying 64 electrodes 1.5 m apart and adopting a Wenner–Schlumberger configuration. Seismic noise signals were recorded by two arrays of seismometers (arrays 1 and 2, Fig. 2.), when the excavation had reached a depth of 7.5 m. Height 30s period three component CMG40T Guralp seismometers were deployed in circular arrays with apertures ranging from 8 to 40 m. The recording time of seismic noise was about an hour for each array.

3. RESULTS FROM ELECTRICAL RESISTIVITY PROFILES, SPT ANALYSIS AND SOIL ANALYSIS

The inversion of apparent resistivity values for the two profiles E1 and E2 was performed using the software RES2DINV with the L1 norm (Loke and Barker, 1996). The two electrical images (Fig. 3.) were obtained after 5 and 6 iterations with a RMS of 4.5 to 5.7 %. For the chosen configuration, the penetration depth is 17 m. In Fig. 3., the locations of neighboring boreholes and seismic arrays are indicated. The images show that the range of electrical resistivity (ρ) is very spread out between 1 Ωm to 1100 Ωm, which indicates a large variability in the electrical properties of alluvial materials. Both E1 and E2 profiles show a surface layer (2-3 m thick) highly resistive (ρ> 400 Ωm). The excavation of the land has shown that this weaker layer is composed of coarse alluvium comprising pebbles, located below the water table. Locally this layer shows significant decreases in resistivity (10 Ωm between 12m and 16.5m along E2), resulting from lateral variations in lithology with the appearance of finer facies (pockets of clay).

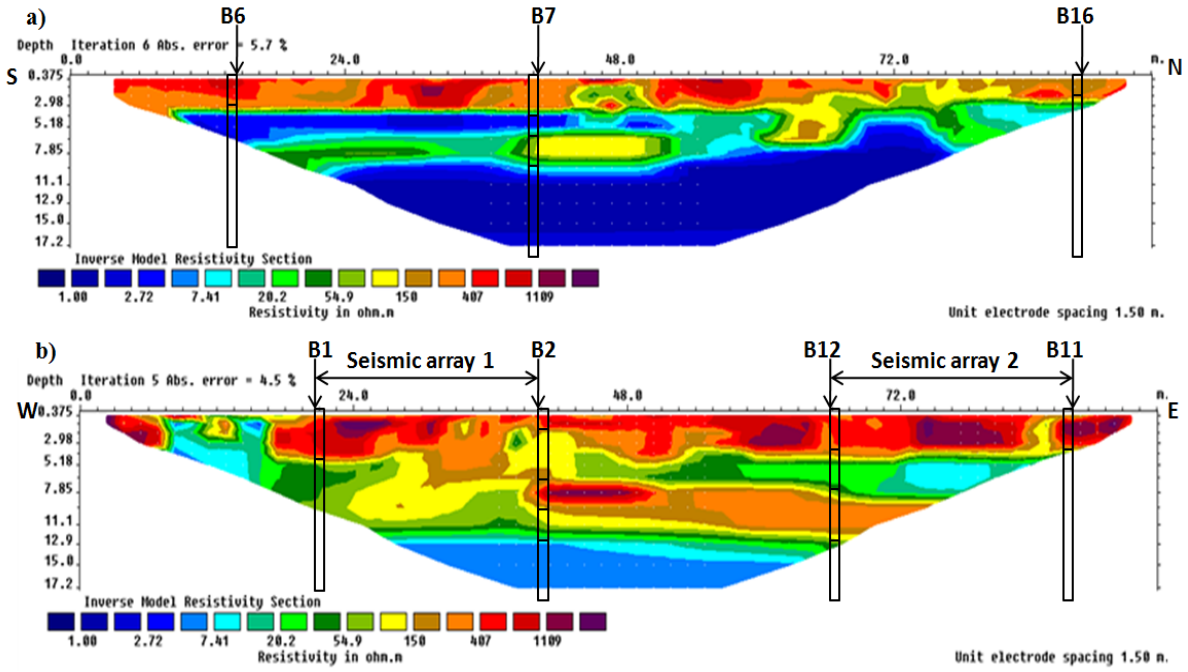

Figure 3. Electrical profile with the location of boreholes for a) E1 and b) E2 profiles

Under this rough surface layer, the resistivity generally decreases, indicating the presence of finer or saturated soils. The electrical resistivity of profile E1 (Fig. 3.a.) is generally very low (ρ <10 Ωm) up to 17 m depth). This highly conductive ground is probably a layer of clay that is interbedded in a coarser level of 2-3 m thickness with an electrical resistivity between 50 and 150 Ωm. Against by the electrical image of the profile E2 (Fig. 3.b) shows a more complex structure, with a horizontal stratigraphy disturbed by lateral variations in resistivity. A conductive layer (ρ <10 Ωm), which may be clay, appears at 10-11 m depth and locally at the end East of the profile E2.

A geological interpretation of the two electrical images was performed using the SPT penetration tests and tests carried out occasionally on grain size distribution of samples taken from boreholes (Fig. 4.). Fig. 4. exhibits curves of penetration testing N (z) measured in seven boreholes located along the electrical profiles, and the type of soil (USCS International Classification) determined by sieve analysis. The review of profile E2 data, shows that the conductive layer encountered at 12 m depth, is a sandy clay or clayey sand with a penetration resistance relatively small (N <20) except in the borehole B2. From the results of SPT and soil classification, this layer should not exceed 5 m thick. The overlying layers are more resistive (ρ >20 Ωm) and resistant (N >30). They correspond to the presence of beds of gravel or sand. According to sieve analysis, the conductive surface layer encountered at a depth of 4 m at the end east of the profile consists of sandy loam. The same distinctions can be made on the profile E1: the conductive layer is characterized by its clay (clayey sand) while the more resistive land are generally more compact and coarse. A geological interpretation of the data set is proposed in Fig. 4., identifying the following lands: clay formation (ρ> 10 Ωm), silty formation (ρ = 20 to 90 Ωm) to gravelly sandy formation (ρ = 90 400 Ωm) and pebble formation (ρ = 400-1100 Ωm). Fig. 4 shows both the vertical variability (stratification) and horizontal (lateral facies variations) of alluvial layers. The top of the clay layer, located at 12-13 m depth, approaches to within 5 m of the surface W at the end of the site.

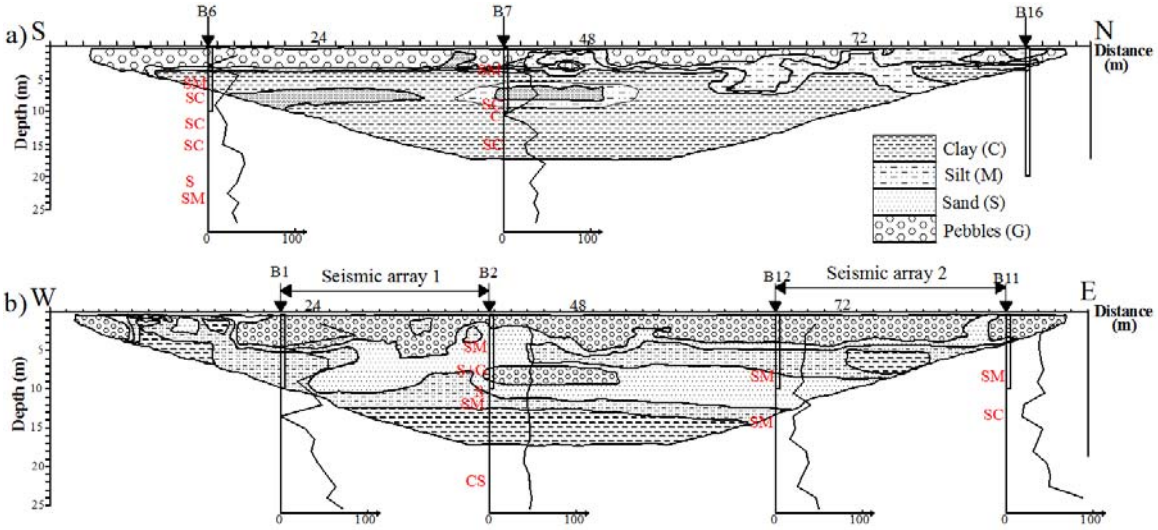

Figure 4. Interpretative cross section along the electrical profiles with the values N (SPT) along profiles a) E1 and b) E2. The results of sieve analysis are shown in red. G: Gravel, S: Sand, M: Silt & C: Clay (USCS classification).

4. EXTRACTION OF SHEAR-WAVE VELOCITIES THROUGH AMBIENT SEISMIC NOISE MEASUREMENTS

Seismic noise windows were processed using the frequency-wave number and spatial autocorrelation methods (Wathelet et al, 2008) in order to derive the Rayleigh wave dispersion curves, which are shown in Fig. 5a with the error bars. The use of the two methods and several array apertures allowed covering the frequency range from 3.5 Hz to 22 Hz. The phase velocity dispersion curves were then inverted to obtain shear wave velocity (Vs) vertical profiles, applying the Conditional Neighborhood algorithm (Wathelet, 2008). All treatments were performed with the software Geopsy (Wathelet et al., 2008). The inversion of the dispersion curve of Rayleigh waves do not provide a unique solution, and the choice of the parameterization (number of layers, range of velocity, and thickness values for the layers) is of prime importance for obtaining reliable results (Renalier et al., 2010). The electrical and SPT results suggest the presence of a few meters thick soft clayey layer, which top depth can vary from a few meters to more than 10 m (Fig. 5c). Because of the trapping of energy below an overlying stiffer layer, the effective dispersion curve can migrate to higher modes (Socco and Strobbia 2004). The best fit (Fig. 5a and b) was obtained by considering that the low and high frequency parts of the

dispersion curve correspond to the first higher and fundamental modes, respectively. The combined interpretation of all the geotechnical and geophysical data yields the following layered structure below array 2, from top to bottom: (1) a 8 m thick relatively stiff layer of gravel to silty sand with Vs = 500

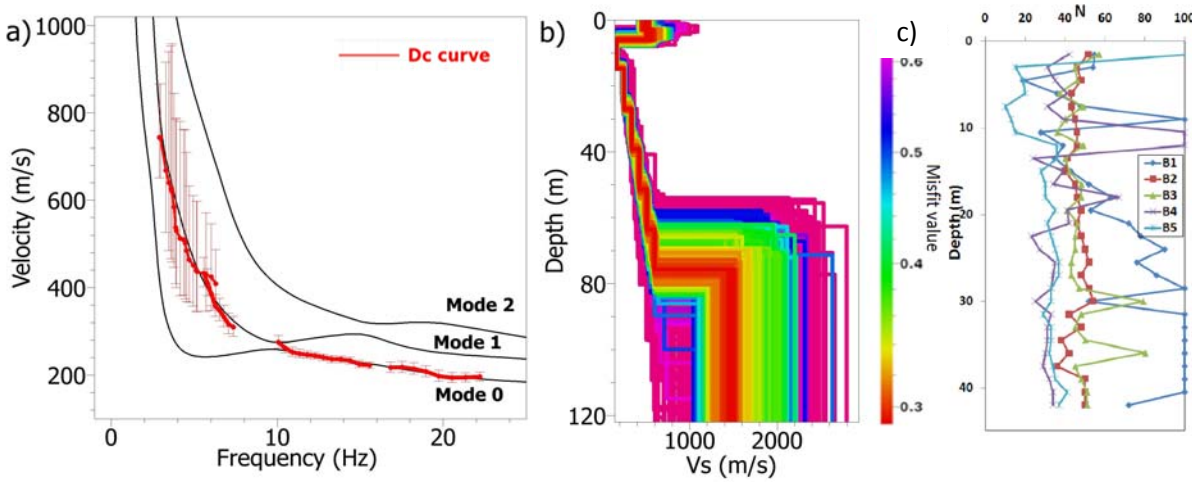

Figure 5. a) Phase velocities of Rayleigh waves measured at array 2 (red dots) with error bars, and the dispersion curves of the three first modes computed from the best inverted Vs profile. b) Vs profiles at array 2. c) Standard penetration resistance (SPT) N values measured in the vicinity of array 2. The zero value on the depth axis is 2 m deeper than on electrical tomography.

m/s, (2) a 10 m thick low velocity layer (Vs < 200 m/s) of clay, (3) more than 55 m of sand, in which linearly Vs increases from 200 m/s to 600 m/s, (4) the bedrock (Vs> 1000m/s) reached at a depth of 70-80 m.

5. RELATION BETWEEN VS AND N-SPT

Several researchers have proposed relationships between Vs and penetration resistance N for different soil types (Sykora and Stokoe, 1983). Empirical relationships for the sand are displayed in Fig. 6a together with average values obtained in this study for the sand layer that occurs at depths larger than 15 m. The average and standard deviation values of N (z) were derived by averaging values obtained at 4 to 5 boreholes close to each seismic array (Fig. 5c and 6c). The mean and standard deviation of Vs (z) at each depth were obtained from the ensemble of 1000 statistically acceptable Vs profiles explaining the data within their uncertainty bounds (Lomax and Snieder, 1994; Souriau et al., 2011). Vs-N values obtained in this study are in agreement with the predictive values (Brandenberg and Naresh, 2010). However, the large data dispersion leads to a low correlation (R = 0.33), most probably as a result of the large uncertainty on the N values (Fig. 6b).

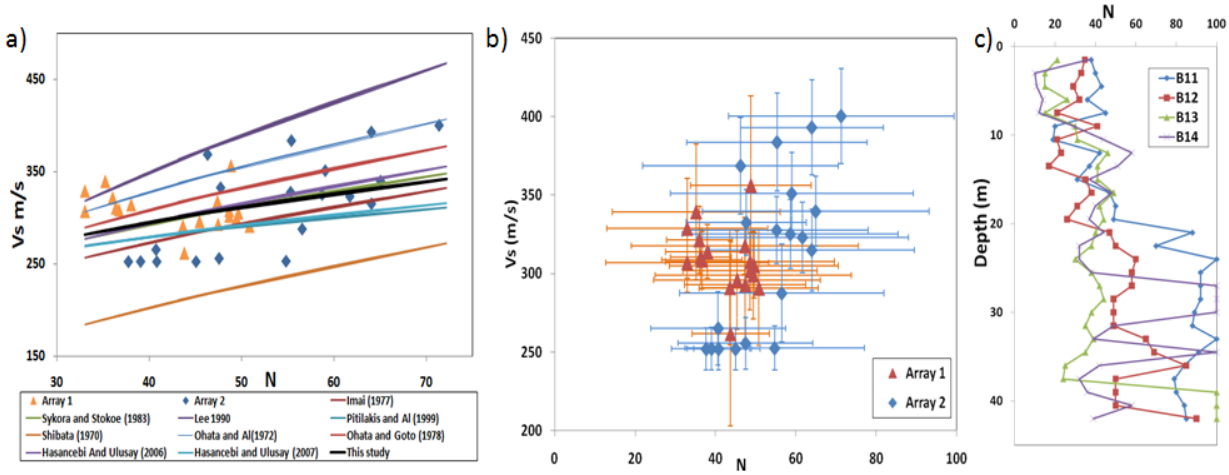

Figure 6. a) Average values of Vs as a function of average values of N (SPT) in the deep sand for sites 1 and 2, together with Vs-N relationships found in the literature. b) Average Vs and N values with their error bars. c) Sandard penetration resistance N measured at 5different SPT tests conducted close to array 1.

6. SPATIAL VARIABILITY OF SOIL

6.1. Definition And Modelling

Due to the spatial inherent variability in soils and the uncertainties in the measurement process, soil properties typically vary with the location of in-situ test and soil samples. The complex soil formation process determines the extent of homogeneity of soil properties. Sampling from adjacent locations in a relative homogeneous soil mass produce similar results with variation. Therefore, soil properties can be effectively described by their correlation structure within the framework of random fields (Vanmarcke, 1983).

The soil uncertainties and variability can be modeled as random variable or random fields. The random variables are defined by a probability density function (the mean μ, the standard deviation σ and a probability distribution) and a correlation can exist between two random variables. When modeling the spatial variability of the soil properties as a random field, each property is represented by a probability density function and an autocorrelation function described by the vertical or horizontal scale of fluctuation (autocorrelation distance). This function represents the degree of dependence of two values for the same property at two distinct points of the ground.

An important and necessary statistical parameter for representing the natural variability of soil properties is the scale of fluctuation also called autocorrelation distance. In fact, the autocorrelation functions are a useful indicator of dependencies as a function of distance in time or space, and they can be used to assess the distance required between sample points for the values to be effectively uncorrelated. In the one dimensional case, Table1 presents a list of common correlation structures with their autocorrelation distances, showing the autocorrelation function and the corresponding correlation distance (Popescu, 1995):

Table 1. Common one-dimensional correlation structures

Model	Autocorrelation Function	Autocorrelation Distance
Squared Exponential	$e^{-\left(\frac{\tau}{a}\right)^2}$	$a\sqrt{\pi}$
Triangular	$\begin{cases} 1-\frac{\lvert\tau\rvert}{a} & \text{si } \lvert\tau\rvert \le a \\ 0 & \text{si } \lvert\tau\rvert > a \end{cases}$	a
Exponential	$e^{\frac{-\lvert\tau\rvert}{a}}$ (a>0)	$\frac{2}{a}$
Cosine Decaying	$e^{-b\tau}\cos a\tau$	$\frac{2b}{b^2+a^2}$

In Table 1, the term τ represents the space lag vector or the separation distance between two different locations where the value of a specific soil parameter is following a certain random field. In other words, the autocorrelation function shown above is used to evaluate the correlation between the values of a certain parameter of soil at two different locations.

To ensure that the autocorrelation distance (θ) of a random field obtained for a certain soil type is meaningful and reflect well the soil variability, it is necessary that the sampling distance s is less than half the autocorrelation distance $s < \theta / 2$ (Popescu 1995).

6.2. Data Analysis

The statistical analysis of a random field, representing a soil property, is achieved through the determ-

ination of the mean, standard deviation, probability density function and the autocorrelation function of this field. The probability density function (pdf) of a sample data is estimated using least square method through fitting the sample probability density function (pdf) to an existing pdf type that gives least values of error on its parameters; this procedure is simply done using the distribution fitting tool in MATLAB. But, in general, it is well known in geotechnical engineering domain that the probability density function of data related to soil parameters follows a lognormal distribution.

The autocorrelation function estimation follows the same procedure as for the determination of the pdf type. From the measurements of an equidistant survey of Δu, the estimate of the value of the autocorrelation function between two values of the property separated by u_j can be obtained by the following formula (Popescu, 1995):

$$\rho(u_j) = \frac{1}{\bar{\sigma}^2 n}\sum_{i=1}^{n-j+1}(x_{i-}\bar{\mu}_x)(x_{i+j-1}-\bar{\mu}_x) \quad (1)$$

Where n is the number of measurements of the soil property, j=0 ... n, x_i is the value of the property measured at the distance $i\Delta u$ and $\bar{\mu}_x$ and $\bar{\sigma}_x$ are respectively the mean and standard deviation of the estimated property. Once the sample autocorrelation function is evaluated, a fitting procedure using MATLAB program is followed to determine the autocorrelation structure, from existing models shown in Table1, which best fits the sample autocorrelation function. This fitting process, using the least square method, gives two important outputs, the coefficient of determination (R^2) which provides a measure of how well new values are likely to be predicted by the fitting autocorrelation function and the parameters of the fitting autocorrelation function used to determine the autocorrelation distance of the field.

6.3. Results

A statistical analysis performed on the geophysical and geotechnical data is presented and discussed. The PDF, mean, standard deviation and autocorrelation structure of the shear wave velocity, electrical resistivity and SPT profiles are calculated and best fitted to an existing statistical model.

6.3.1 Best fitted PDF

For the shear wave velocity, using data from all available profiles of arrays 1 and 2, it was observed that the lognormal probability density function best fits the Vs data probability distribution as one can see from Fig. 7.a. The errors on the mean and standard deviation between the obtained histogram and the fitted PDF were found respectively equal to 4.8% and 3.4%. The same analysis was performed on the electrical resistivity and the SPT data, and it was found that the data histograms of ρ and N (SPT) were best fitted to the lognormal probability distribution similar to Vs with small errors on the mean and standard deviation.

6.3.2 Autocorrelation structure

The autocorrelation structure in the vertical and horizontal directions of all the measured soil parameters are determined for the sand and clay layers. Based on equation (1), it was found that all the parameters were best fitted to the cosine decaying autocorrelation function as one can observe from figs. 7.b. and 8. The R^2 values obtained was found greater than 0.92. Fig. 7.b. shows the fitted autocorrelation function with the sample autocorrelation functions of Vs profile of array 2. The vertical autocorrelation distance was found equal to 3.585 m for the sand layer and 0.7817 m for the clay layer which means that the clay layer is more spatially variable than the sand layer with respect to Vs.

Fig 8.a. shows the fitted autocorrelation function with the sample autocorrelation functions of BH13. It was found that the autocorrelation distance is found around 2m for the sand layer and smaller than 0.5 m for the clay layer. However since the sampling distance for the SPT is 1.5 m which is smaller than half the autocorrelation distance, the sampling distance for the SPT does not reflect well the soil

variability as previously explained. The statistical analysis of all the remaining boreholes close to BH13 has shown similar results.

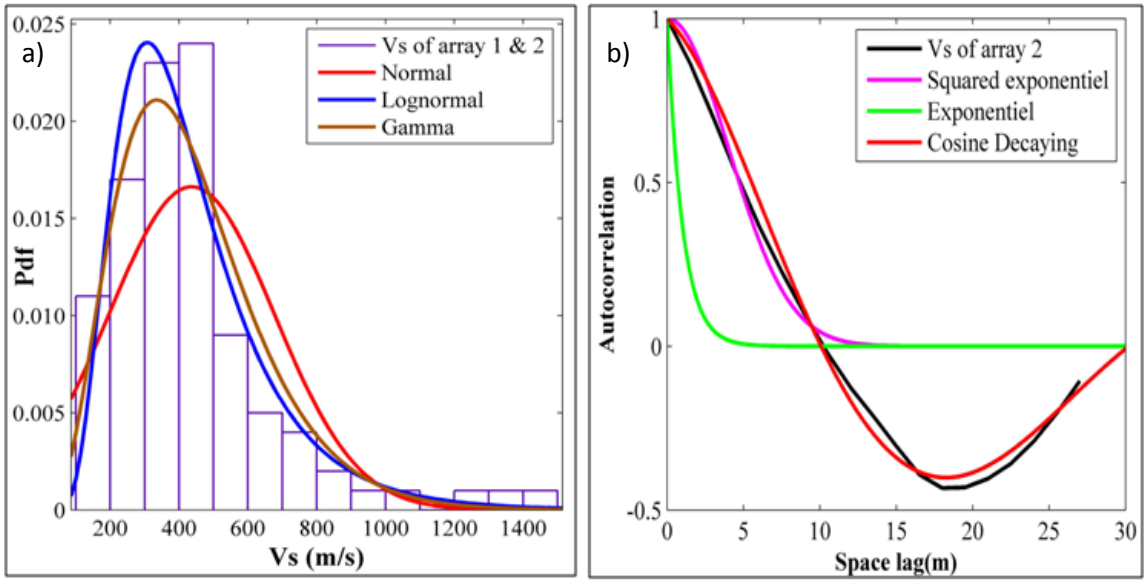

Figure 7. a) Probability density function of measured Vs values (histogram) represented by the histogram and the various theoretical statistical laws; b) Fitted autocorrelation function for Vs in sand layer

Fig 8.b. shows the fitted autocorrelation function with the sample autocorrelation functions of resistivity profiles. The horizontal autocorrelation distances were analyzed for this case since the lateral variability can only be quantified from the 2D electrical images. However, it cannot be measured from Vs and SPT due to the lack of horizontal sampling distances. It was found that the value of the horizontal autocorrelation distance for resistivity is around 7.5 m in the sand layer and around 5 m in the clay layer.

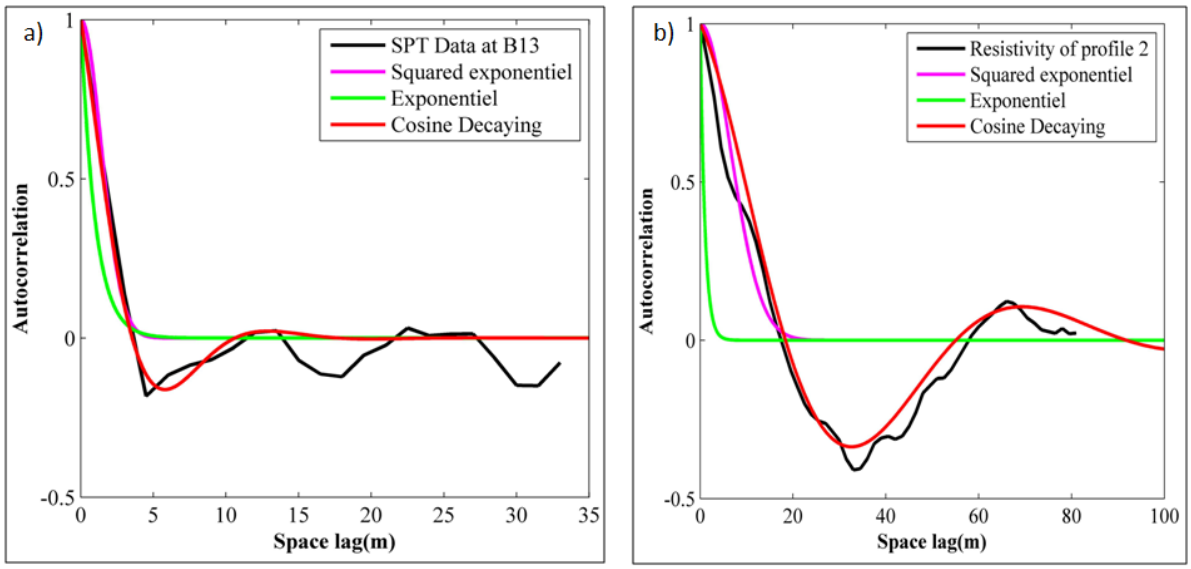

Figure 8. a) Fitted autocorrelation function for SPT data at borehole B13 in sand layer. b) Fitted autocorrelation function for resistivity in the sand layer

7. CONCLUSION

Geophysical and geotechnical tests were carried out in the 13500 m² lot 4748 in Beirut. The combined analysis of geotechnical and geophysical data (boreholes logs and standard penetration test values N-SPT, electrical resistivities and shear wave velocities) has shown a stratified media composed, from top to bottom, of a rigid surface layer of gravels and pebbles of 3 m thickness overlaying a 8 meters thick sandy/silty layer, then a soft clay layer of few meters thickness, and finally a thick layer of sand with increasing resistance. Besides, electric resistivity profiles locally calibrated by geotechnical information have evidenced large lateral heterogeneity within the first 20 meters. Although widely dispersed and wikely correlated, the values of Vs and N determined in the deep layer of sand are in agreement with the empirical Vs-N relationships found in literature.

For the quantification of the soil spatial variability, we have found that the lognormal distribution have best fitted the histograms of all the soil parameters (N, resistivities, Vs). From the autocorrelation structures, it was observed that the clay layer is more variable than the sand layer in both vertical and horizontal directions.

Finally, the combination of geophysical images and parameters, geotechnical data, and geological data will enable us to assess a consistent 3D geotechnical and geophysical model accounting for spatial variability and input parameter uncertainty.

ACKNOWLEDGMENTS

This work is partially funded by project LIBRIS ANR Risknat-006 and Institut de Recherche pour le Developpement (IRD). Seismic instruments used in this study belong to the French national pool of portable seismic instruments Sismob (INSU-CNRS).

REFERENCES

Abdallah, C. (2007). Application de la télédétection et des systèmes d'informations géographiques à l'étude des mouvements de terrain au Liban, Ph. D. thesis, Paris 6.

Andrus, R. D.; Piratheepan, P.; Ellis, B. S.; Zhang, J. & Juang, C. H. (2004). Comparing liquefaction evaluation methods using penetration-VS relationships, Soil Dynamics and Earthquake Engineering 24(9-10), 713 – 721.

Brandenberg Scott, J., Bellana, N. and Shantz, T. (2010). Shear Wave Velocity as a Statistical Function of Standard Penetration Test Resistance and Vertical Effective Stress at Caltrans Bridge Sites, Technical Report Documentation.

Cho, S. (2007). Effects of spatial variability of soil properties on slope stability. Engineering Geology 92 ,97–109

Dubertret,L. (Juin 1944) Carte de Beyrouth et Environs.

Finn, W., (2000). State-of-the-art of geotechnical earthquake engineering practice: Soil Dynamics and Earthquake Engineering, 20, 1-15.

Foti, S., Parolai, S., Albarello, D., Picozzi, M. (2011). Application of Surface-Wave Methods for Seismic Site Characterization. Surveys in Geophysics, 32, 6, 777-825.

Hasancebi, N. & Ulusay, R. (2007). Empirical correlations between shear wave velocity and penetration resistance for ground shaking assessments, Bulletin of Engineering Geology and the Environment 66(2), 203--213.

Jaksa, M., Brooker, P. and Kaggwa, W. (1997). Modeling the spatial variability of the undrained shear strength of clay soils using geostatstics. Geostatistics Wollongong 96, Volume 2, 1284-1295.

Jongmans, D. & Garambois, S. (2007), Geophysical investigation of landslides: a review, Bulletin de la Société Géologique de France 178(2), 101-112.

Lomax, A., and Snieder R. (1994). Finding sets of acceptable solutions with a genetic algorithm with application to surface wave group dispersion in Europe. Geophysical Research Letters 21, 2617–2620.

Loke, M.H., Barker, R.D.(1996). Rapid least-squares inversion of apparent resistivity pseudo sections by a quasi-Newton method. Geophysical Prospecting 44, 131–152.

Oh, S. and Sun, C-G. (2008). Combined analysis of electrical resistivity and geotechnical SPT blow counts for

the safety assessment of fill dam, Environ Geol 54:31–42.
Popescu, R. (1995). Stochastic variability of soil properties: data analysis, digital simulation, effects on system behaviour. PhD thesis, Princeton University, Princeton, NJ.
Popescu,R., Prevost, J.H & Decodatis, G. (1997). Effects of spatial variability on soil liquefaction: some design recommendations. Geotechnique 47, 1019-1036
Renalier F., Jongmans D., Savvaidis A., Wathelet M., Endrun B. and Cornou C. (2010). Influence of parameterization on inversion of surface wave dispersion curves and definition of an inversion strategy for sites with a strong Vs contrast, Geophysics 75, B197 (2010); doi:10.1190/1.3506556.
Socco, L. V., and Strobbia, C. (2004). Surface-wave method for near-surface characterization: a tutorial: Near Surface Geophysics, 2, 165–185.
Souriau, A., Chaljub , E., Cornou, C., Margerin, L., Calvet, M., Maury, J., Wathelet, M., Ponsolles, C., Grimaud, F., Péquegnat, C., Langlais, M., Guéguen, P. (2011). Multimethod characterization of the French Pyrenean valley of Bagnères-de-Bigorre for seismic hazard evaluation: observations and models, Bull seism. Soc. Am., 101(4): 1912–1937, doi: 10.1785/0120100293
Sykora, D. E., and Stokoe, K. H. (1983). Correlations of in-situ measurements in sands of shear wave velocity, Soil Dyn. Earthq. Eng., 20, 125–36.
Vanmarcke, E., et Grigoriu, M. (1983). Stochastic finite element analysis of simple beams." Journal of Engineering Mechanics, 109(5), 1203-1214.
Wathelet, M. (2008). An improved neighborhood algorithm: parameter conditions and dynamic scaling. Geophysical Research Letters, 35, L09301, doi:10.1029/2008GL033256
Wathelet, M., Jongmans, D., Ohrnberger, M. and Bonnefoy-Claudet, S. (2008). Array performances for ambient vibrations on a shallow structure and consequences over Vs inversion. Journal of Seismology, 12, 1-19.
Youssef Abdel Massih, D., Harb, J. and Soubra, A.-H. (2009). Reliability analysis of Lebanese slopes subjected to seismic loads. 2nd international conference on Computational Methods in Structural Dynamics and Earthquake Engineering, Island of Rhodes, Greece, 22-24 June 2009, 18p.